RESEARCH ARTICLE | JANUARY 24 2024

Optimization algorithm to generate a robust magnetic force of the magnetic navigation system against position error of a magnetic robot

Special Collection: 68th Annual Conference on Magnetism and Magnetic Materials

D. Lee ; J. Kwon ; G. Jang

AIP Advances 14, 015240 (2024)
https://doi.org/10.1063/9.0000648

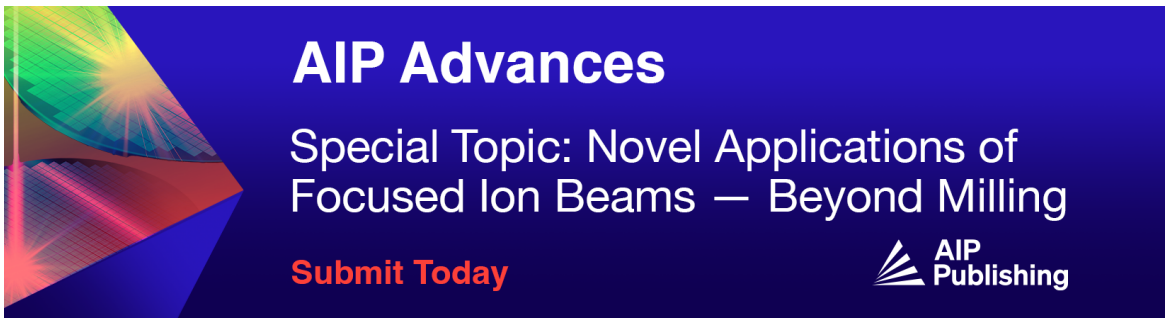

Optimization algorithm to generate a robust magnetic force of the magnetic navigation system against position error of a magnetic robot

Cite as: AIP Advances 14, 015240 (2024); doi: 10.1063/9.0000648
Submitted: 27 September 2023 • Accepted: 20 November 2023 •
Published Online: 24 January 2024

D. Lee, J. Kwon, and G. Jang[a)]

AFFILIATIONS

PREM, Department of Mechanical Engineering, Hanyang University, Seoul 04763, Republic of Korea

Note: This paper was presented at the 68th Annual Conference on Magnetism and Magnetic Materials.
[a)]**Author to whom correspondence should be addressed:** ghjang@hanyang.ac.kr

ABSTRACT

We propose an optimization algorithm to generate a robust magnetic force against position error to achieve good controllability of the magnetic robot in the region of interest of a magnetic navigation system comprising electromagnets. We formulate an optimization problem that minimizes the norm of the spatial derivatives of the magnetic force subject to the constraints of the magnetic flux density and magnetic force. The robust magnetic force generated by the proposed algorithm was compared with conventional pseudo-inverse matrix method and verified through an experiment in which a magnetic robot was successfully steered along a bifurcated glass tube to reach a target position.

I. INTRODUCTION

Occlusive vascular disease is caused by stenosis of the major arteries in the body, including those in the brain and heart. To treat occlusive vascular disease, endovascular intervention is conducted. In a conventional endovascular intervention, medical doctors utilize guidewires and catheters to manually access the clogged lesion. Subsequently, complicated procedures, such as tunneling, ballooning, and stent installation, are performed. Magnetic robots (MRs) used for a robotic endovascular intervention have been investigated as a promising alternative to conventional manual endovascular intervention.[1,2] The magnetic torque and force to actuate the MR can be generated by the interaction between an external magnetic field and the permanent magnet inside the MR such that the MR can reach a target lesion or perform therapeutic functions remotely. The external magnetic field can be generated and controlled by a magnetic navigation system (MNS), which is classified as permanent magnet (PM) type or electromagnet (EM) type.[3] The PM-type MNS generates a magnetic field by mechanically moving PMs, with which it is difficult to generate a time-varying magnetic field, such as a rotating magnetic field, in real time. Alternatively, the EM-type MNS generates a magnetic field by applying and controlling the current flowing through EMs. This type of MNS has the advantage of easily generating a time-varying magnetic field and easily turning the magnetic field on and off. However, these EM-type MNSs simultaneously produce a lot of heat, which limits the maximum available magnetic flux density. To increase the magnetic flux density of these MNSs, some researchers have inserted magnetic cores or connected them to a back yoke. This type of MNS can generate a strong magnetic flux density by using the highly permeable magnetic core. However, it is difficult to produce a uniform magnetic gradient within the region of interest (ROI) of this type of MNS[4,5] To generate the perfectly uniform magnetic gradient, nine components of the spatial derivatives of the magnetic gradient should be zero. The spatial derivatives of the magnetic gradient depend on the shape and configuration of the EMs of the MNS. In most cases, a non-uniform magnetic gradient is generated because of the non-zero components of the spatial derivatives such that an unintended magnetic force may be generated if there is a difference between the expected and actual position of the MR. This unintended magnetic force may ultimately result in loss of MR control.

We propose an optimization algorithm to generate a robust magnetic force against position error to achieve good controllabil-

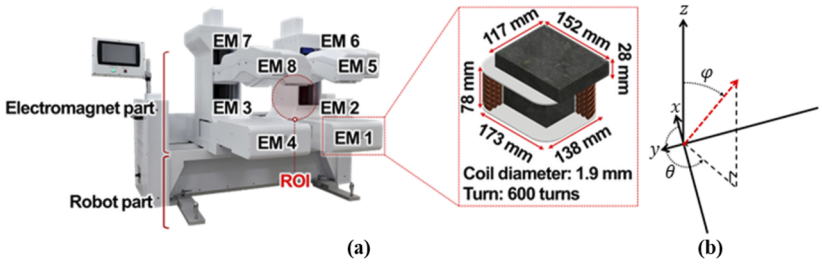

FIG. 1. (a) EM-type MNS with eight cores and (b) the direction (θ, φ) of the magnetic force.

ity of the MR in the ROI of the EM-type MNS with a magnetic core. We formulate an optimization problem that minimizes the norm of the spatial derivatives of the magnetic force subject to the constraints of the magnetic flux density and magnetic force. We applied the proposed method to an MNS with eight electromagnets, as shown in Fig. 1(a).[6] In the electromagnet part, each tip of the eight electromagnets corresponds to each vertex of the ROI. The robustness of the magnetic force generated by the proposed algorithm was compared with that of a prior method and was verified by successfully steering an MR along a bifurcated glass tube to reach a target lesion.

II. OPTIMIZATION ALGORITHM TO GENERATE A ROBUST MAGNETIC FORCE

The magnetic flux density and magnetic force generated by the EM-type MNS with a core can be represented as follows:[7,8]

$$\begin{bmatrix} \mathbf{B} \\ \mathbf{F} \end{bmatrix} = \begin{Bmatrix} \mathbf{A_B}(P) \\ \mathbf{A_F}(\mathbf{m}, \mathbf{P}) \end{Bmatrix} \cdot \mathbf{I} = \mathbf{A}(\mathbf{m}, \mathbf{P}) \cdot \mathbf{I} \tag{1}$$

where $\mathbf{A_B}(\mathbf{P})$ and $\mathbf{A_F}(\mathbf{m}, \mathbf{P})$ represent the actuation matrices of the magnetic flux density and magnetic force, respectively, and $\mathbf{m}$ and $\mathbf{P}$ represent the magnetic dipole moment and the position of interest $\mathbf{P} = (x, y, z)$. As shown in Fig. 1(b), the desired direction of the magnetic field and magnetic force can be calculated after determining the values of θ and φ. It leads to four constraints because there are two constraints (θ and φ) for the magnetic flux density and magnetic force. Thus, the dimension of the null space of the actuation matrix $(\mathbf{A}(\mathbf{m}, \mathbf{P}))$ of our EM-type MNS is 4 (= 8 − 4). Finally, the general current solution vectors $\mathbf{I}$ to generate the magnetic field and force can be calculated as follows:

$$\mathbf{I} = \mathbf{I_p} + \sum_{k=1}^{4} \mathbf{null_k}(\mathbf{A}) \cdot c_k \tag{2}$$

where $\mathbf{I_p}$ is a particular current solution vector that generates the desired magnetic flux density and magnetic force, $\mathbf{null_k}(\mathbf{A})$ is the k-th basis vector that forms the null space of the actuation matrix $\mathbf{A}$, and c_k are the free variables. Prior researchers have determined the current vector that generates the desired magnetic flux density and magnetic force at the position of interest by calculating the pseudo-inverse of the actuation matrix.[7,8]

To evaluate the uniformity of the magnetic force, we introduced the vector $\mathbf{GF}$ comprising the spatial derivatives of the magnetic force as follows:

$$\mathbf{GF}(\mathbf{m}, \mathbf{P}) = \left[\frac{\partial F_x}{\partial x} \; \frac{\partial F_y}{\partial x} \; \frac{\partial F_z}{\partial x} \; \frac{\partial F_x}{\partial y} \; \frac{\partial F_y}{\partial y} \; \frac{\partial F_z}{\partial y} \; \frac{\partial F_x}{\partial z} \; \frac{\partial F_y}{\partial z} \; \frac{\partial F_z}{\partial z} \right]^T. \tag{3}$$

We formulated an optimization problem to generate a robust magnetic force against position error to achieve good controllability of the MR in the ROI of our EM-type MNS as follows:

$$\begin{gathered} \text{Find } I_n \text{ to minimize } \|\mathbf{GF}(\mathbf{m}, \mathbf{P})\| \\ \text{subject to } \|\mathbf{B}\| \geq \|\mathbf{B_{target}}\|, \\ \|\mathbf{F}\| \geq \|\mathbf{F_{target}}\| \text{ and } I_n \leq I_{supply} \quad (n = 1, \ldots, 8) \end{gathered} \tag{4}$$

where $\|\mathbf{B_{target}}\|$, $\|\mathbf{F_{target}}\|$, and I_{supply} are the magnetic flux density to steer the MR to the desired direction, the magnetic force to move the MR to the desired position, and the maximum available current (12 A) of the power supply, respectively. The specific values of $\mathbf{B_{target}}$ and $\mathbf{F_{target}}$ depend on the shape of MR described in Sec. III. The optimization problem of Eq. (4) can be solved by using the interior-point algorithm of fmincon solver in MATLAB.

III. RESULTS AND DISCUSSION

Figures 2(b)–2(d) shows the distribution of the magnetic flux density and the magnetic force as determined by the pseudo-inverse matrix and the proposed method to generate a B_x of 1 mT and F_y of 5 mN at the position of interest (0, 0, 0), respectively. Table I shows the values of the magnetic flux density and magnetic force at the origin and at four vertices of a square with a length of 20 mm. As shown in Fig. 2 and Table I, the magnetic flux density and magnetic force from the pseudo-inverse matrix method are very sensitive to position error with respect to the position of interest. However, the proposed method generates a magnetic flux density and magnetic force robust against position error.

To verify the robustness of the proposed method, an experiment was conducted using a radially magnetized cylinder-shaped MR with a diameter of 3 mm and length of 10 mm. We set the value of B_{target} and F_{target} in Eq. (4) to be 1 mT (experimentally determined) and 5 mN (weight of MR) to stably steer the MR. In the experiment, the MR was controlled to move along the path rep-

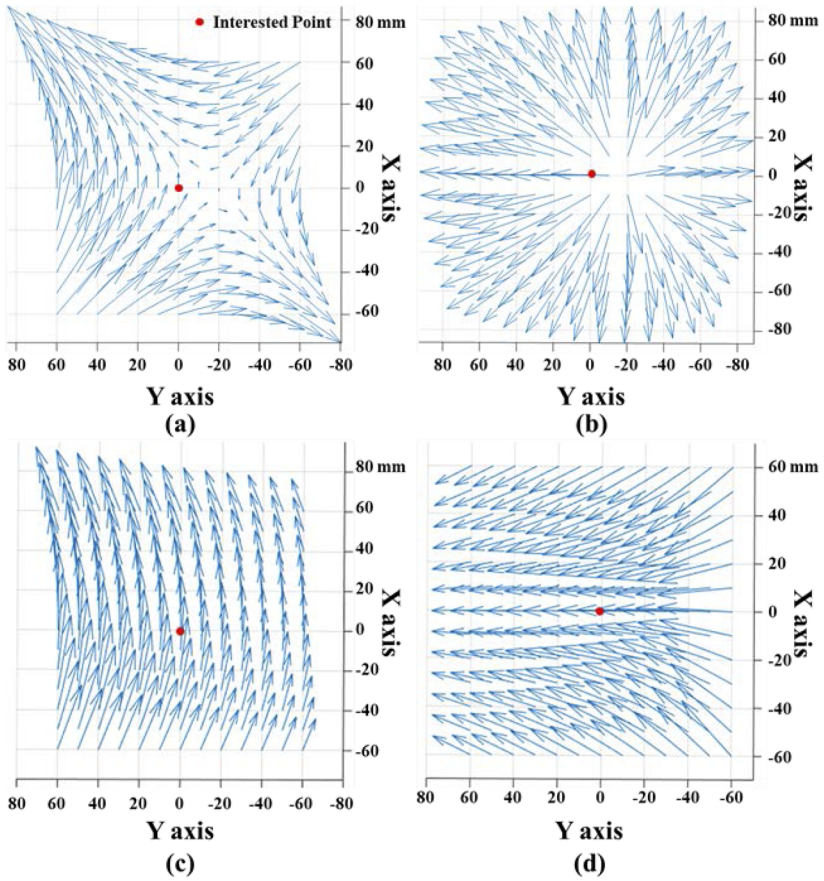

FIG. 2. Distribution of the (a) magnetic flux density and (b) magnetic force when the pseudo-inverse matrix method was applied. Distribution of the (c) magnetic flux density and (d) magnetic force with application of the proposed method.

TABLE I. Magnetic flux density and magnetic force from the pseudo-inverse matrix method and the proposed method.

Point (mm)	Pseudo-inverse matrix method				Proposed method			
	B_x (mT)	B_y (mT)	F_x (mN)	F_y (mN)	B_x (mT)	B_y (mT)	F_x (mN)	F_y (mN)
(0, 0)	3	0	0	5	3	0	0	5
(20, 20)	3.6	1.3	1	2	4.8	1.3	0	5
(20, −20)	1.1	1.3	2	−2	2.3	1.3	0	5
(−20, 20)	3.7	−1.3	−1	2	4.7	−1.3	0	5
(−20, −20)	1.1	−1.3	−3	−1	2.1	−1.2	0	5

resented by the red line in Fig. 3(a), starting from Point ① and ending at Point ⑦, inside a 7-mm-diameter glass tube filled with water. Table II shows the magnetic force applied to the MR from the pseudo-inverse matrix method and the proposed method along the target path. The magnetic force was calculated and applied at each point from ① to ⑥ to control the MR along the target path, and the magnetic force at the middle points from ①* to ⑥*, which are points between each path from ① to ⑦, was the change of the magnetic force according to position. The pseudo-inverse matrix method and the proposed method generate similar magnetic force from ① to ⑥; however, the magnetic force from the pseudo-inverse matrix method changes more rapidly with position than does that from the proposed method. As shown in the rows corresponding to ④ and ④*, the y-component of the magnetic force from the pseudo-inverse

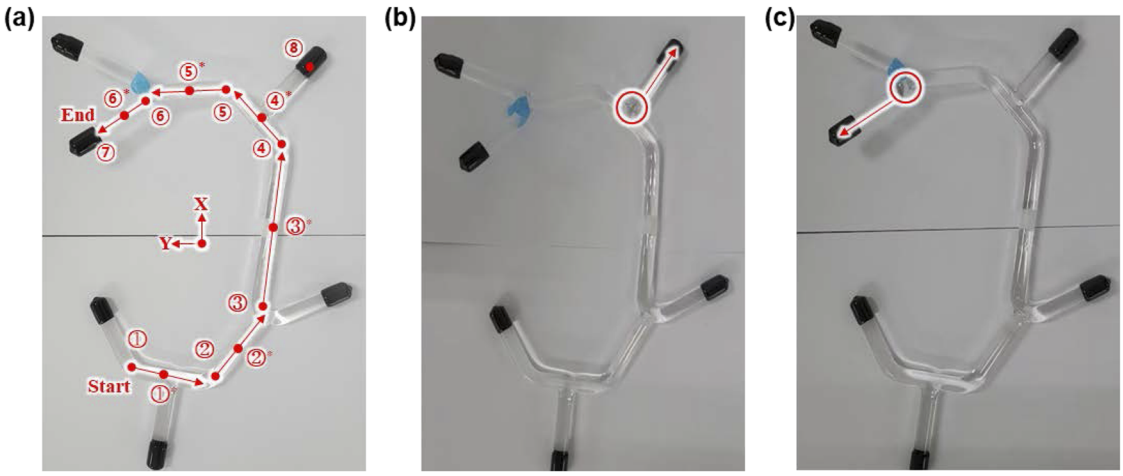

FIG. 3. (a) Experimental setup and targeted path of the MR along a glass tube. (b) With the pseudo-inverse matrix method, the MR reached point ⑧ after deviating from the targeted path. (c) With the proposed method, the MR was successfully steered to the target position. (Multimedia view available online.)

TABLE II. Magnetic force from the pseudo-inverse matrix method and the proposed method along the targeted path.

		Pseudo-inverse matrix method			Proposed method		
Point	X, Y, Z (mm)	F_x (mN)	F_y (mN)	F_z (mN)	F_x (mN)	F_y (mN)	F_z (mN)
①	(−100,30,0)	0.00	−5.00	0.00	0.00	−5.00	0.00
①*	(−100,0,0)	0.31	−6.27	0.48	0.00	−5.02	0.00
②	(−100, − 30,0)	4.36	−2.44	0.00	4.42	−2.48	0.00
②*	(−80, − 40,0)	5.93	−3.96	0.11	4.45	−2.72	0.00
③	(−50, − 50,0)	5.00	0.00	0.00	5.31	0.00	0.00
③*	(0, − 50,0)	4.42	−0.14	1.72	5.44	−0.10	0.00
④	(50, − 50,0)	3.19	3.76	0.83	3.23	3.80	0.84
④*	(70, − 35,10)	3.44	−0.86	0.21	3.34	3.77	1.01
⑤	(85, − 20,15)	−0.92	4.75	1.28	−0.94	4.86	1.30
⑤*	(80,10,20)	0.45	4.13	1.48	−0.61	5.41	1.44
⑥	(75,35,25)	−3.14	3.68	1.25	−3.20	3.75	1.28
⑥*	(70,50,30)	−2.14	2.66	1.55	−3.35	3.83	1.35

matrix method changes its direction in addition to generating a z-component of the magnetic force. As shown in Fig. 3(b) using the pseudo-inverse matrix method, the MR deviated from the control path at Point ④ and unintentionally reached Point ⑧, leading to loss of control by the generated magnetic force, as in Table II.

However, when the proposed method was used to generate the magnetic force as shown in Fig. 3(c), the MR was stably controlled from ① to ⑦ despite the position change. This experiment verifies that our proposed method generates robust magnetic force against position error so that the MR can be stably propelled along the desired path. This experiment was videotaped and is attached to this paper. (Multimedia view).

IV. CONCLUSION

We proposed an optimization algorithm to generate a robust magnetic force against the position error of a magnetic robot for an EM-type MNS. Our proposed method minimizes the norm of the vector comprising nine spatial derivatives of the magnetic force such that the variation of the magnetic force with respect to the position error is minimized. With the application of our proposed method, the MR can more stably move along the targeted path in the glass tube than that using the conventional pseudo-inverse method. We performed an experiment with an MR moving in a complicated glass tube and validated the robustness of the proposed method. This research will enhance control of MRs using magnetic forces.

ACKNOWLEDGMENTS

This research was supported by a grant of the National Research Foundation of Korea funded by the Korean government (MSIT) (Grant No. 2023R1A2C2005143).

AUTHOR DECLARATIONS

Conflict of Interest

The authors have no conflicts to disclose.

Author Contributions

D. Lee: Conceptualization (lead); Formal analysis (lead); Software (lead); Writing – original draft (lead). **J. Kwon**: Formal analysis (supporting); Investigation (supporting); Validation (supporting); Visualization (supporting). **G. Jang**: Funding acquisition (lead); Project administration (lead); Supervision (lead); Writing – review & editing (lead).

DATA AVAILABILITY

The data that support the findings of this study are available from the corresponding author upon reasonable request.

REFERENCES

[1] Q. Wang, X. Du, D. Jin, and L. Zhang, ACS Nano **16**, 604 (2022).
[2] B. J. Nelson, S. Gervasoni, P. W. Y. Chiu, L. Zhang, and A. Zemmar, Proceedings of the IEEE **110**, 1028 (2022).
[3] Z. Yang and L. Zhang, Advanced Intelligent Systems **2**, 2000082 (2020).
[4] X. Du, L. Yang, J. Yu, K. F. Chan, P. W. Y. Chiu, and L. Zhang, *2020 5th International Conference on Advanced Robotics and Mechatronics (ICARM)* (2020), Vol. 125.
[5] L. Yang, M. Zhang, H. Yang, Z. Yang, and L. Zhang, *2021 IEEE/RSJ International Conference on Intelligent Robots and Systems (IROS)* (IEEE, 2021), pp. 7476.
[6] W. Lee, Ph D. thesis, Hanyang University, 2021.
[7] M. P. Kummer, J. J. Abbott, B. E. Kratochvil, R. Borer, A. Sengul, and B. J. Nelson, IEEE Trans. Robot **26**, 1006 (2010).
[8] S. Schuerle, S. Erni, M. Flink, B. E. Kratochvil, and B. J. Nelson, IEEE Transactions on Magnetics **49**, 321 (2013).